

LEARNING AUDIO-VISUAL EMBEDDING FOR PERSON VERIFICATION IN THE WILD

Peiwen Sun^{1,2}, Shanshan Zhang², Zishan Liu¹, Yougen Yuan²,
Taotao Zhang², Honggang Zhang¹, Pengfei Hu²

¹School of Artificial Intelligence,
Beijing University of Posts and Telecommunications, Beijing, China
²TEG AI, Tencent Inc, Beijing, China

ABSTRACT

It has already been observed that audio-visual embedding is more robust than uni-modality embedding for person verification. Here, we proposed a novel audio-visual strategy that considers aggregators from a fusion perspective. First, we introduced weight-enhanced attentive statistics pooling for the first time in face verification. We find that a strong correlation exists between modalities during pooling, so joint attentive pooling is proposed which contains cycle consistency to learn the implicit inter-frame weight. Finally, each modality is fused with a gated attention mechanism to gain robust audio-visual embedding. All the proposed models are trained on the VoxCeleb2 dev dataset and the best system obtains 0.18%, 0.27%, and 0.49% EER on three official trial lists of VoxCeleb1 respectively, which is to our knowledge the best-published results for person verification.

Index Terms— person verification, audio-visual, cycle consistency

1. INTRODUCTION

Biometrics-based person verification technologies are widely used in access control. In the wild, the speech segments are corrupted with real-world noise including laughter, music, and other sounds. Similarly, face images have variations in pose, image quality, and motion blur. It creates additional challenges for the verification system.

The development of verification in Voxceleb [1, 2] first appeared in speaker verification. The research [3] proposed attentive statistics pooling to focus on important frames of speaker verification and get higher discriminative ability than the traditional averaging method. In further research, ECAPA-TDNN [4] was based on blocks of TDNNs and Squeeze-Excitation(SE) [5] to reconstruct frame-level features. Meanwhile, The margin-based softmax loss originating from face recognition is widely used for training models [6–9]. These losses were also customized to adapt to the speaker verification task [10, 11] and achieved SOTA at that time.

The performance of speaker systems would degrade dramatically under wild circumstances [12]. To solve the problem, researchers have found that simply fusing the scores

from speaker embeddings and facial embeddings can yield good results [13, 14]. For the first time, S. Shon [12] attempted to fuse audio-visual information with deep learning-based models to achieve better results. As the transformer has been proposed, it seemed more efficient [15] to fuse different modalities in large datasets. Previous studies have sought implicit feature expression and supervision patterns from the perspective of network structure. To further explore the explicit correlations, Y. Liang [16] gave person verification a point of view of the HGR maximal correlation. Most of the research on audio-visual works [15, 17] still focused on extracting frame-level embeddings and then simply averaging them as an aggregator to get segment-level embeddings.

To further increase aggregator robustness and generalization of utterance level embedding, our network is reconsidered from a fusion perspective and brings a huge leap forward in VoxCeleb. As a prerequisite, we enhance the frame weight of the attention statistics pooling [3] to adjust the situation of the audio-visual training process. Intuitively, facial muscles and syllables of pronunciation have a mutual impact on this task. Then, cycle consistency [18] was introduced into the aggregator for the inference of the keyframes of two modalities. The method that combines weight-enhanced attentive statistics pooling and cycle consistency is called joint attentive pooling. Each frame contributes according to its relevance to the final face representation avoiding equal contributions and preventing accumulated errors. Finally, as an analysis, visualization maps are generated to explain how this system interacts between modalities and why it is effective.

2. METHOD

The overall network (Fig.1) consists of the backbone of each modality (Sec.3), joint attentive pooling module, and fusion module (Sec.2.3). The joint attentive pooling module is the combination of weight-enhanced attentive statistical pooling in Sec.2.1 and cycle consistency learning Sec.2.2

2.1. Weight-enhanced attentive statistical pooling

The data of each modality are pre-processed as stated in Sec.3 and sent to the respective encoders. But when visual information is added for joint training, there is a serious drop. To solve the problem, we introduce weight enhanced method of

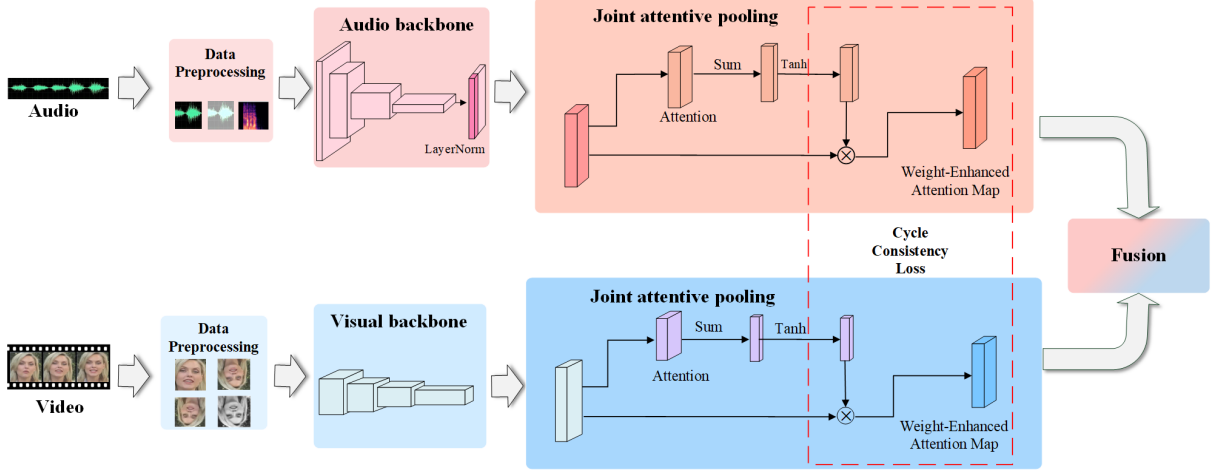


Fig. 1. Overall Network

attentive statistical pooling, which is proved to play a positive role in many aspects in the later comparison experiment. The detailed calculation process of weight enhanced method is as follows.

Through the original attentive statistical pooling mechanism [4], each frame will be given different weights.

$$e^{t,c} = (\mathbf{v}^c)^T \tanh(\mathbf{W}h^t + \mathbf{b}) + k^c, \quad (1)$$

where h^t denotes the activations of the last frame layer at time step t . The parameters $\mathbf{W} \in \mathbb{R}^{R \times C}$ and $\mathbf{b} \in \mathbb{R}^{R \times 1}$ project the information for self-attention into a smaller \mathbb{R} -dimensional representation that is shared across all C channels to reduce the parameter count and risk of overfitting.

This information is transformed to a channel-dependent self attention score through a linear layer with weights $\mathbf{v}^c \in \mathbb{R}^{R \times 1}$ and bias k^c .

However, here comes a problem. It is found that the value of temporal attention λ_t has a comparatively small standard deviation. That is to say, the keyframes in the time domain are not obvious. To make the attention more bifurcated and to help the learning of the subsequent layers, we enhance the weight of each frame by the following equation.

$$e_{\tanh}^{t,c} = e^{t,c} * \frac{\lambda_{\tanh}^t}{\lambda^t}, \quad (2)$$

while the attention map $e^{t,c} \in \mathbb{R}^{T \times A}$ and the projected attention map $e_{\tanh}^{t,c} \in \mathbb{R}^{T \times A}$ is given by

$$\lambda^t = \text{sum}_{\text{temporal}}(e^{t,c}), \quad (3)$$

$$\lambda_{\tanh}^t = \text{mu}(\lambda^t) * \tanh\left(\frac{\lambda^t - \text{mu}(\lambda^t)}{\text{std}(\lambda^t)}\right) + \text{mu}(\lambda^t). \quad (4)$$

$\text{mu}(\cdot)$, $\text{std}(\cdot)$ is mean and standard deviation of the matrix, $\lambda^t \in \mathbb{R}^{T \times 1}$ denotes the temporal attention; The activated weights are projected into a more dispersed and polarized space $\mathbb{R}^{T \times 1}$ and preserve the mean. If not, fine-grained granularity brings the difficulties of convergence for further experiments. The activation method can avoid non-convergence, alleviate overfitting and be beneficial to the later learning of audio-visual weight interactions.

So compared to the original attention map, it is using the new map $e_{\tanh}^{t,c}$ instead of the original map $e^{t,c}$. This scalar score $e_{\tanh}^{t,c}$ then normalized over all frames by applying the softmax function channel-wise across time:

$$\alpha^{t,c} = \frac{\exp(e_{\tanh}^{t,c})}{\sum_{\tau} \exp(e_{\tanh}^{\tau,c})}. \quad (5)$$

The self-attention score $\alpha_{t,c}$ represents the importance of each frame given the channel and is used to calculate the weighted statistics of channel c . Then the weighted mean vector and weighted standard deviation vector can be calculated as

$$\tilde{\mu}^c = \sum_t \alpha^{t,c} h^{t,c}, \quad (6)$$

$$\tilde{\sigma}^c = \sqrt{\sum_t \alpha^{t,c} (h^{t,c})^2 - (\tilde{\mu}^c)^2}. \quad (7)$$

2.2. Cycle consistency learning

From the perspective of face verification, researchers such as [19] hope to eliminate the impact of facial expressions on face verification. Meanwhile, from the perspective of speaker verification, some speech information of audio interval is not helpful for speaker verification. Then there is a natural idea, hoping to establish some potential probability relationships of keyframes between the face verification and speaker verification, which is called the ‘‘complementary rule’’.

Essentially, we want to build a network where keyframes between different modalities can be derived from each other. And naturally, there comes a loop. The network used to construct the supervised loop is two encoders consisting of 3-layer mlp to encode the weights of simple temporal frames.

Here we generalize adversarial loss and cycle consistency loss into regression tasks (Fig.2). Red and blue blocks represent the temporal attention belonging to different modes respectively, while the solid and dashed lines represent the temporal attention under real conditions and the predicted temporal attention respectively. The adversarial loss follows the previous paper [18] to serve a similar purpose, but it is not really adversarial. It ensures each encoder can evolve smoothly,

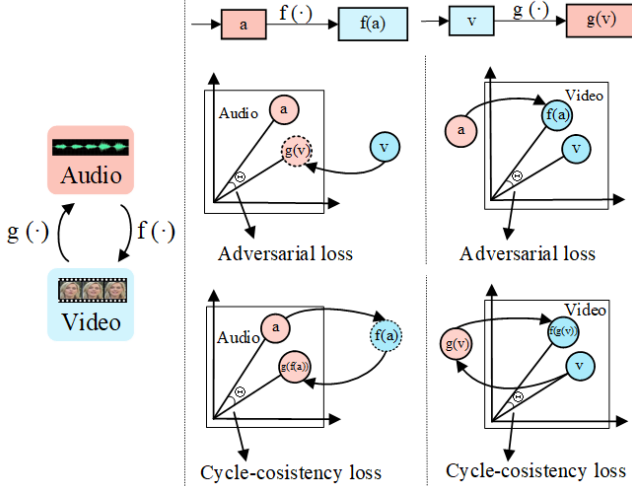


Fig. 2. Proposed adversarial loss and cycle consistency loss

which means the encoder can produce more realistic temporal weights. The cycle consistency loss ensures that temporal weights from different sources in the same modality have the same intensity.

Adversarial loss and cycle consistency loss only involve the mapping of temporal attention λ_{tanh}^t , and we express the objective as:

$$\mathcal{L}_{adv} = 2 - \langle a, g(v) \rangle - \langle v, f(a) \rangle, \quad (8)$$

$$\mathcal{L}_{cycle} = 2 - \langle v, f(g(v)) \rangle - \langle a, g(f(a)) \rangle, \quad (9)$$

$$a = \lambda_{tanh}^{t,a}, v = \lambda_{tanh}^{t,v}, \quad (10)$$

while $g(\cdot)$ and $f(\cdot)$ represent 2 MLP encoders separately, \mathcal{L}_{adv} and \mathcal{L}_{cycle} denote adversarial loss and cycle consistency loss, $\langle \cdot, \cdot \rangle$ is the cosine similarity operator.

Each direction of the loop generates 2 losses which force the attentive statistics pooling to learn potential information.

Therefore, the overall loss can be calculated as

$$\mathcal{L} = \mathcal{L}_{AAM} + \beta \mathcal{L}_{adv} + \gamma \mathcal{L}_{cycle}, \quad (11)$$

while \mathcal{L}_{AAM} is AAM softmax loss, β and γ are constants that are used to control and adjust the weights of different losses. And their values can be determined by training experience.

Compared with the L2 loss, cosine distance is more concerned with the angular relationship between vectors than their absolute size. Using cosine distance as the loss can make the inferred position of the keyframe more accurate. In this case, the unnormalized cosine distance is often better than the Euclidean distance to give the optimal solution.

2.3. Fusion strategy

Simple Soft Attention Fusion [20] is implemented. But we use the fully connected layer instead of the transformer layer in the original model to achieve the best fusion effect of the model.

For the joint embedding generated by the network, the convergence can be accelerated by some tricks during the training process. We follow [21] to impose an orthogonality constraint on the fused embeddings. We hold the point of view that it is mainly used to accelerate convergence.

3. EXPERIMENT SETUP

VoxCeleb1&2 [1, 2] are used in our experiment. VoxCeleb is an audio-visual dataset consisting of 2,000+ hours of short human speech clips extracted from interview videos on YouTube. For model training, we use the development set of VoxCeleb2, which contains 5,994 speakers. To better evaluate the performance of our network, we adopt 3 trials in VoxCeleb1. For audio data, 80-dimensional Fbank features are extracted with a 25 ms window and 10 ms frameshift, and augmentation with the random mask is added along both the time and frequency domain. Then we do the cepstral mean on the Fbank features. The MUSAN [22] and RIR Noise datasets [23] are used as noise sources and room impulse response functions, respectively. For each video segment, we extracted 6 fps in VoxCeleb1 [1] and 25 fps in VoxCeleb2 [2] datasets. Then use the similarity transformation to map the face region to the same shape ($1 \times 128 \times 128$), which means that we use grey images instead of RGB. Finally, we normalize each image's pixel value to reside in the range of $[-0.5, 0.5]$. The advanced face detection methods [24, 25] and datasets [26, 27] are wilder and more fine-grained. So face detection and face alignment are not employed during pre-processing since rough face detection has been performed in VoxCeleb datasets. [1, 2].

For the audio encoder, we use ECAPA-TDNN [4] into which Fbank feature is fed to extract speaker embedding. We made only a few changes to ECAPA-TDNN, which adds additional scale information to the second layer. For the visual encoder, the face feature is extracted by the IResNet18 backbone same as [6].

The training process is divided into two stages. Two different modalities are trained separately first and then finetune in the overall network. All models are trained using AAM softmax loss with a margin of 0.5 and a scaling factor of 30 with 32 NVIDIA Tesla P40s. We use the SGD optimizer with an initial learning rate of 0.01 and decrease the learning rate by 50% every 2 epochs. As an experimental result, β and γ are set to 1 and 0.5. Weight decay is set to $5e-4$ to avoid overfitting and the global batch size is 320.

We use cosine distance with adaptive s-norm [28] for scoring. Then we report the Equal Error Rate (EER) and minimum Detection Cost Function (minDCF) with $P_{target} = 0.01$ and $C_{FA} = C_{Miss} = 1$ for performance evaluation.

4. RESULT ANALYSIS

From table 1, we observe that the weight-enhanced method for unimodality will not bring obvious changes to speech while using activation in the face alone can be a relief for the generalization pressure of attentive statistic pooling. And the later experiments show that the activation operation on a single modality brings better performance on the joint audio-visual model. In terms of vision alone, compared with the results of works [15, 17], our proposed method uses less image information (grey image instead of RGB), less data preparation (without face detection and face alignment), a

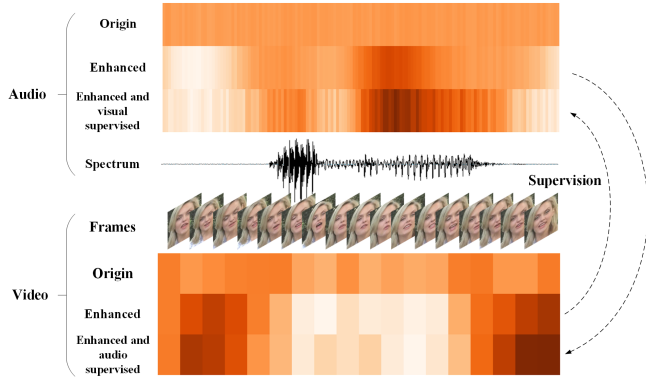


Fig. 3. Attention Heatmap of a 0.8-sec video clip

shallower extractor (IResNet18 instead of ResNet34 [15] or SE-ResNet50 [17]). This method enables us to gain a competitive reduction of EER to 63.7% of the previous baseline of vision by adopting a higher sampling rate.

The cycle-consistency loss will finally converge to around 0.03-0.05. As the loss converges and each encoder is analyzed separately, the transformation from vision to audio is easier to converge than the transformation from audio to vision. This shows that the “complementary rule” is mainly reflected in “vision-supervised audio”. From the results in Table 1, the use of cycle loss indeed enhances the weight of important time frames. Compared to audio-visual person verification, the fusion network alone can greatly reduce the EER down to 30.7% of the previous baseline. The simple score ensemble of multiple systems is still valid for this experiment. The best results are achieved after a simple score ensemble.

Attention map Fig.3 of the output of the two different layers is generated to verify the “complementary rule”. We can intuitively see that the time frame weight is adjusted adaptively and the two modalities are roughly complemen-

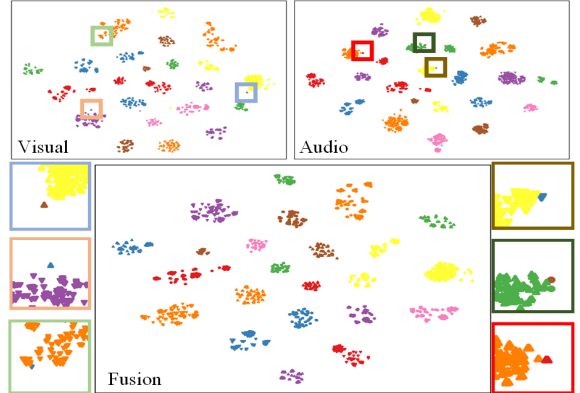


Fig. 4. Sample visualization

tary. The most accurate time frame for face verification is often accompanied by rare facial muscle movements; while the most accurate time frame for speaker verification is often accompanied by a wide range of facial muscle movements.

About 20 hard samples were selected from the VoxCeleb1-H dataset for t-SNE dimensionality reduction visualization analysis. It can be seen from Fig.4 that each diagram of a single modality can easily find 5-6 outliers. But our network is more robust to these outliers. This phenomenon well demonstrates the robustness of the proposed network.

5. CONCLUSION

Generally, we proposed a novel audio-visual strategy that considers aggregators from a fusion perspective. Compared with previous aggregators, we proposed joint attentive pooling based on cycle consistency as a generic aggregator for the first time. It significantly reduces the EER down to 28.0% of the popular systems. And analysis shows the robustness of our network and the existence of “complementary rules”. In future work, the audio-visual unsupervised pretrain model will be explored to reach a higher level.

Table 1. Performance of proposed network

Type	Architecture	#Modality	VoxCeleb1-O		VoxCeleb1-E		VoxCeleb1-H	
			EER(%)	MinDCF	EER(%)	MinDCF	EER(%)	MinDCF
Unimodal	ECAPA-TDNN [4]	A	0.87	0.107	1.12	0.132	2.12	0.210
		SimAM-Resnet [29]	A	0.64	0.067	0.84	0.089	1.49
	Z. Chen [17]	①A	2.31	-	2.23	-	3.78	-
		②V	2.26	-	1.54	-	2.37	-
		③fusion	0.59	-	0.43	-	0.74	-
		ensemble(①,②)	0.51	-	0.43	-	0.78	-
	ensemble(①,②,③)	0.50	-	0.38	-	0.68	-	
Audio-visual	Y. Qian [15]	A	1.62	-	1.75	-	3.16	-
		V	3.04	-	2.18	-	4.23	-
		fusion	0.71	-	0.48	-	0.85	-
	Ours	A w/o enhanced†	0.98	0.140	1.24	0.163	2.30	0.264
		④A	0.99	0.140	1.24	0.163	2.27	0.264
		V w/o enhanced†	2.59	0.214	1.88	0.198	3.39	0.297
		⑤V	1.44	0.147	1.28	0.157	2.14	0.230
		fusion w/o cons†	0.22	0.022	0.27	0.035	0.52	0.058
		⑥fusion	0.18	0.017	0.26	0.035	0.49	0.057
	Audio-visual	Ours	ensemble(④,⑤,⑥)	0.14	0.012	0.21	0.028	0.37

† “w/o cons” means “without cycle consistency” and “w/o enhanced” means “without weight enhanced method”.

6. REFERENCES

- [1] A. Nagrani, J. S. Chung, W. Xie, and A. Zisserman, "Voxceleb: Large-scale speaker verification in the wild," *Computer Science and Language*, 2019.
- [2] J. S. Chung, A. Nagrani, and A. Zisserman, "Voxceleb2: Deep speaker recognition," in *INTERSPEECH*, 2018.
- [3] K. Okabe, T. Koshinaka, and K. Shinoda, "Attentive statistics pooling for deep speaker embedding," *arXiv preprint arXiv:1803.10963*, 2018.
- [4] B. Desplanques, J. Thienpondt, and K. Demuynck, "Ecapa-tdnn: Emphasized channel attention, propagation and aggregation in tdnn based speaker verification," in *Interspeech*, pp. 3830–3834, 2020.
- [5] J. Hu, L. Shen, and G. Sun, "Squeeze-and-excitation networks," in *Proc. CVPR*, pp. 7132–7141, 2018.
- [6] J. Deng, J. Guo, N. Xue, and S. Zafeiriou, "Arcface: Additive angular margin loss for deep face recognition," in *Proc. CVPR*, June 2019.
- [7] Y. Huang, Y. Wang, Y. Tai, X. Liu, P. Shen, S. Li, J. Li, and F. Huang, "Curricularface: adaptive curriculum learning loss for deep face recognition," in *Proc. CVPR*, pp. 5901–5910, 2020.
- [8] W. Liu, Y. Wen, Z. Yu, M. Li, B. Raj, and L. Song, "Sphereface: Deep hypersphere embedding for face recognition," in *Proc. CVPR*, pp. 212–220, 2017.
- [9] H. Wang, Y. Wang, Z. Zhou, X. Ji, D. Gong, J. Zhou, Z. Li, and W. Liu, "Cosface: Large margin cosine loss for deep face recognition," in *Proc. CVPR*, pp. 5265–5274, 2018.
- [10] L. Wan, Q. Wang, A. Papir, and I. L. Moreno, "Generalized end-to-end loss for speaker verification," in *Proc. ICASSP*, pp. 4879–4883, IEEE, 2018.
- [11] X. Xiang, S. Wang, H. Huang, Y. Qian, and K. Yu, "Margin matters: Towards more discriminative deep neural network embeddings for speaker recognition," in *APSIPA ASC*, pp. 1652–1656, IEEE, 2019.
- [12] S. Shon, T.-H. Oh, and J. Glass, "Noise-tolerant audio-visual online person verification using an attention-based neural network fusion," in *Proc. ICASSP*, pp. 3995–3999, IEEE, 2019.
- [13] S. O. Sadjadi, C. S. Greenberg, E. Singer, D. A. Reynolds, L. P. Mason, J. Hernandez-Cordero, *et al.*, "The 2019 nist audio-visual speaker recognition evaluation.," in *Odyssey*, pp. 259–265, 2020.
- [14] J. Alam, G. Boulianne, L. Burget, M. Dahmane, M. D. Sánchez, A. Lozano-Diez, O. Glembek, P.-L. St-Charles, M. Lalonde, P. Matejka, *et al.*, "Analysis of abc submission to nist sre 2019 cmn and vst challenge.," in *Odyssey*, pp. 289–295, 2020.
- [15] Y. Qian, Z. Chen, and S. Wang, "Audio-visual deep neural network for robust person verification," *IEEE. Trans Audio Speech Lang Process*, vol. 29, pp. 1079–1092, 2021.
- [16] Y. Liang, F. Ma, Y. Li, and S.-L. Huang, "Person recognition with hgr maximal correlation on multimodal data," in *Proc. ICPR*, pp. 1–8, IEEE, 2021.
- [17] Z. Chen, S. Wang, and Y. Qian, "Multi-modality matters: A performance leap on voxceleb.," in *INTERSPEECH*, pp. 2252–2256, 2020.
- [18] J.-Y. Zhu, T. Park, P. Isola, and A. A. Efros, "Unpaired image-to-image translation using cycle-consistent adversarial networks," in *Proc. CVPR*, pp. 2223–2232, 2017.
- [19] J. Chang, Z. Lan, C. Cheng, and Y. Wei, "Data uncertainty learning in face recognition," in *Proc. CVPR*, pp. 5710–5719, 2020.
- [20] Y.-H. H. Tsai, S. Bai, P. P. Liang, J. Z. Kolter, L.-P. Morency, and R. Salakhutdinov, "Multimodal transformer for unaligned multimodal language sequences," in *Proc. ACL*, vol. 2019, p. 6558, NIH Public Access, 2019.
- [21] M. S. Saeed, M. H. Khan, S. Nawaz, M. H. Yousaf, and A. Del Bue, "Fusion and orthogonal projection for improved face-voice association," in *Proc. ICASSP*, pp. 7057–7061, 2022.
- [22] D. Snyder, G. Chen, and D. Povey, "Musan: A music, speech, and noise corpus," *arXiv preprint arXiv:1510.08484*, 2015.
- [23] T. Ko, V. Peddinti, D. Povey, M. L. Seltzer, and S. Khudanpur, "A study on data augmentation of reverberant speech for robust speech recognition," in *Proc. ICASSP*, pp. 5220–5224, IEEE, 2017.
- [24] J. Deng, J. Guo, E. Ververas, I. Kotsia, and S. Zafeiriou, "Retinaface: Single-shot multi-level face localisation in the wild," in *Proc. CVPR*, 2020.
- [25] J. Guo, J. Deng, A. Lattas, and S. Zafeiriou, "Sample and computation redistribution for efficient face detection," in *Proc. ICLR*, 2021.
- [26] S. Yang, P. Luo, C. C. Loy, and X. Tang, "Wider face: A face detection benchmark," in *Proc. CVPR*, 2016.
- [27] X. Zhu, Z. Lei, X. Liu, H. Shi, and S. Z. Li, "Face alignment across large poses: A 3d solution," in *Proc. CVPR*, June 2016.
- [28] P. Matejka, O. Novotný, O. Plchot, L. Burget, M. D. Sánchez, and J. Cernocký, "Analysis of score normalization in multilingual speaker recognition.," in *Interspeech*, pp. 1567–1571, 2017.
- [29] X. Qin, N. Li, C. Weng, D. Su, and M. Li, "Simple attention module based speaker verification with iterative noisy label detection," in *Proc. ICASSP*, pp. 6722–6726, IEEE, 2022.